Front. Chem. Sci. Eng. 2019, 13(3): 444–457
https://doi.org/10.1007/s11705-019-1811-6

REVIEW ARTICLE

Review of plasma-assisted reactions and potential applications for modification of metal–organic frameworks

Tingting Zhao, Niamat Ullah, Yajun Hui, Zhenhua Li (✉)

Key Lab for Green Chemical Technology of Ministry of Education, School of Chemical Engineering and Technology,
Collaborative Innovation Center of Chemical Science and Engineering (Tianjin), Tianjin University, Tianjin 300072, China

© Higher Education Press and Springer-Verlag GmbH Germany, part of Springer Nature 2019

Abstract Plasma catalysis is drawing increasing attention worldwide. Plasma is a partially ionized gas comprising electrons, ions, molecules, radicals, and photons. Integration of catalysis and plasma can enhance catalytic activity and stability. Some thermodynamically unfavorable reactions can easily occur with plasma assistance. Compared to traditional thermal catalysis, plasma reactors can save energy because they can be operated at much lower temperatures or even room temperature. Additionally, the low bulk temperature of cold plasma makes it a good alternative for treatment of temperature-sensitive materials. In this review, we summarize the plasma-assisted reactions involved in dry reforming of methane, CO_2 methanation, the methane coupling reaction, and volatile organic compound abatement. Applications of plasma for modification of metal–organic frameworks are discussed.

Keywords plasma catalysis, methane, carbon dioxide, VOCs, metal–organic frameworks

1 Introduction

Plasma technology has attracted broad interest since its discovery by Crookes in 1879. In 1927, American scientists Langmuir and Tonks introduced the term “plasma” [1]. Since then, plasma has been extensively studied. Plasma, which is the fourth state of matter, is a partially or fully ionized gas consisting of electrons, ions, free radicals, and neutrals [2–5]. According to the discharge energy, plasma systems are classified as thermal plasma or cold plasma. Thermal plasma is in the equilibrium state; the bulk temperature can reach several thousands of degrees Celsius, which is close to the electron temperature. In contrast, cold plasma is in a nonequilibrium state in which the electron temperature is higher than thousands of degrees Celsius, but the bulk temperature remains as low as room temperature [6–11]. Cold plasma has been widely studied because it is easier to generate on either the laboratory or the industrial scale than thermal plasma. Depending on the discharge form, cold plasma can be divided into various types. Dielectric barrier discharge (DBD) is a gas discharge in which an insulating medium is inserted between two discharge electrodes. When a sufficiently high voltage is applied to the electrodes, the gas between them breaks down at or above atmospheric pressure to form a DBD. High-voltage pulse discharge is obtained by applying a direct current high-voltage pulse to an electrode. When the potential on the needle electrode reaches a certain value, the strong electric field near the needle tip causes ionization of the surrounding gas, generating a partial discharge phenomenon. Glow discharge refers to a self-sustained discharge. It can easily be created between two electrodes in low vacuum. Radio-frequency discharge can also be operated at a very low pressure but at high frequencies (several megahertz) to achieve nonequilibrium conditions. Microwave discharge is operated at very high frequencies (e.g., 2.45 GHz) in the microwave range, and therefore, it is far from local thermodynamic equilibrium. Corona discharge occurs when the conductor has a tip with a small radius of curvature. It can be implemented at atmospheric pressure [12–14].

Plasma technology has been widely used in many applications, including reaction facilitation, surface modification, and catalyst preparation [15–19]. Integration of catalysis and plasma has progressed greatly, and plasma-assisted catalysis can provide not only increased activity but also increased stability [11,20–22]. Plasma catalysis is studied in multiple fields such as physical chemistry, catalysis, materials science, plasma physics and chemistry,

---

Received November 20, 2018; accepted December 25, 2018

E-mail: zhenhua@tju.edu.cn

and nanotechnology [23–27]. In this review, we summarize the application of plasma in various catalytic reactions: dry reforming of methane, CO_2 methanation, the coupling reaction of methane, and volatile organic compound (VOC) abatement. In addition, a new type of material, metal–organic frameworks (MOFs), is attracting much attention owing to their relatively high surface areas, well-organized porosities, and tunable chemical structures. The application of plasma for modification of MOFs is also discussed here.

2 Plasma-assisted reactions

2.1 Plasma-assisted methane reforming reaction

Dry reforming of methane proceeds by the following reaction when methane and carbon dioxide are fed into a reactor:

$$\mathrm{CH_4(g) + CO_2(g) \rightarrow 2CO(g) + 2H_2(g)},$$

$$\Delta H^0_{298} = 247\ \mathrm{kJ/mol}.$$

This process is regarded as an effective way to reduce the release of greenhouse gases and synthesize syngas. The regular tetrahedral structure of methane makes activation of the C–H bond (average bond energy of approximately 4.5 eV, i.e., 434 kJ/mol) very difficult. Carbon dioxide, the final product of combustion of carbonaceous material, is also a very stable C1 resource with an average O = C = O bond energy of approximately 5.5 eV, i.e., 532 kJ/mol [28]. Consequently, dry reforming of methane requires a high activation energy, so it is difficult to achieve by traditional catalytic processes. Many researchers have searched for effective solutions in terms of catalyst selection, catalyst carbon deposition behavior, and catalytic mechanism. Moreover, application of various unconventional methods has also been extensively discussed. Among them, plasma technology is thought to be a promising method. Plasma generally plays a role in pretreatment of catalysts, operation of plasma-alone reactors, or operation of combined plasma–catalyst reactors in this catalytic reaction. Many articles have reported work on plasma-pretreated catalysts for dry reforming of methane. They have shown that nonthermal plasma (NTP) may change some of the physicochemical characteristics of the catalyst, giving it higher activity or better performance [15,17–19,21,29–31]. Furthermore, catalytic reactions integrated with plasma can effectively suppress carbon deposition. Ni/Al_2O_3-ZrO_2, Ni/MgAlO, NiPt/MgAlO, NiMgSBA-15, and Co/SiO_2 catalysts pretreated [32] by glow discharge plasma, a Ni/γ-Al_2O_3 catalyst pretreated by DBD plasma [33], and a Pd/TiO_2 catalyst pretreated by radio-frequency plasma [34] all showed improved catalytic performance in dry reforming of methane.

Catalysts may face practical problems such as short lifespan, poor stability, poor carbon deposition resistance, and polluting and time-intensive preparation processes [35–37]. Therefore, plasma-alone reactors without a catalyst are also a focus of research. Tu and Whitehead [38] developed an atmospheric pressure alternating current (AC) gliding arc discharge to synthesize syngas along with value-added carbon nanomaterials, such as spherical carbon nanoparticles, multiwalled carbon nanotubes, and amorphous carbon (Fig. 1). They provided a new method for not only dry reforming of methane but also synthesis of value-added by-products. Moreover, the results revealed that this arc discharge was much more energy efficient than dielectric barrier or corona discharges. Lim and Chun [39] applied a novel plasma converter that had an orifice-type baffle to improve the amount of fed gas and realize greater destruction of CO_2. The CO_2 destruction and CH_4 conversion at a CH_4/CO_2 ratio of 1.29 were 37% and 47%, respectively. Other types of plasma reactors, including DBD reactors, glow discharge reactors, and spark discharge reactors have also been explored for dry reforming of methane [40–42].

Plasma-assisted reactions occur mainly by a free radical mechanism [43,44], and the product selectivity is hard to control. The presence of a catalyst in the plasma system improves the NTP syngas synthesis process. To facilitate

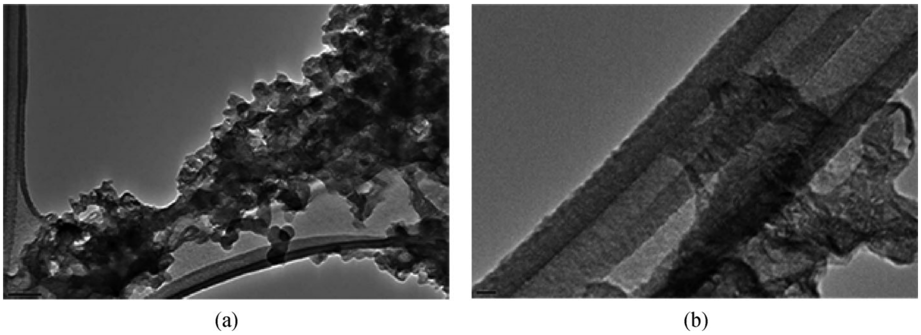
(a) (b)

Fig. 1 Transmission electron microscopy images of carbon produced in the plasma dry reforming process: (a) spherical carbon nanoparticles; (b) carbon nanotubes (CH_4/CO_2 = 7:3, total flow rate: 51 min^{-1}, input power: 165 W). Reprinted from ref. [38], copyright (2014), with permission from Elsevier the NTP dry reforming reaction and enhance its efficiency, various efforts have been made to improve the catalytic performance of this technology. Ray et al. [45] used a glass-bead-packed DBD reactor to obtain 29% conversion of CH_4 and 21% conversion of CO_2 at a specific input energy of 6.4 J/mL. Zhang et al. [46] compared $BaTiO_3$ with other catalysts (glass, Ni/SiO_2, and $NiFe/SiO_2$) in the discharge zone of DBD plasmas. They obtained 16.2% conversion of CO_2 and 27.3% conversion of CH_4 at a plasma power of 86 W. Additionally, the catalytic activity decreased in the sequence $BaTiO_3 > NiFe/SiO_2 > Ni/SiO_2$. Zheng et al. [47] used perovskite $LaNiO_3$ nanoparticles coupled with DBD plasma to explore the kinetics of plasma-catalytic dry reforming of methane. They suggested a global kinetic model considering argon dilution. The model gave satisfactory predictions of plasma-assisted dry reforming of methane over the $LaNiO_3$ catalyst. Chung et al. [48] formed a hybrid plasma photocatalysis system with a spark discharge reactor and a series of perovskite-type photocatalysts to evaluate its effectiveness for methane reforming. They found that plasma played a key role in changing the surface structure of the photocatalyst, which increased the lifetime of electron-hole pairs and thus the syngas generation rate.

Efforts have been made to optimize the plasma-catalytic process because both the plasma setup and reaction conditions strongly influence the yield and energy efficiency. Zhou et al. [41] found that higher methane conversion was obtained at higher discharge powers, and methane conversion increased significantly with the input power below 50 W. Xia et al. [49] varied the gap distance between the electrode from 1.5 to 3.5 mm to investigate the relationship between the distance and the catalytic activity. Similarly, Montoro-Damas et al. [50] systematically investigated the relationship between the gap and the process efficiency. Jin et al. [51] suggested that using an electrode with a large diameter and long discharge gap negatively affected the conversion of CO_2 and CH_4. Other operational parameters including the residence time, input power, frequency, and permittivity have also been widely studied [52–55]. However, despite these attempts, there is still insufficient knowledge and quantitative description of the effect of the operating parameters on the energetic performance.

The high reaction temperature is a serious problem for dry reforming of methane. A thermodynamic analysis of this reaction system was reported in the book “Technology and Application of Plasma” [56]. Because it is a strongly endothermic reaction, methane reforming has to be performed at higher temperature in the conventional catalytic process. Consequently, room-temperature plasma may not yield satisfactory results. Therefore, many researchers have attempted to obtain better catalytic performance by using external heating of the plasma reactor. Yap et al. [57] combined 10% La_2O_3/alumina balls with plasma at room temperature and found that the catalyst was inactive under these conditions. When the reaction temperature was increased from room temperature to 300°C, the CH_4 conversion increased by a factor of almost 3. Sentek et al. [58] tested the effect of temperature (120°C–290°C) on the performance of dry reforming of methane. When a Pd/Al_2O_3 catalyst was used, the methane conversion could reach 50% at 240°C. Kim et al. [59] suggested that activation of C–H bonds can be remarkably improved at temperatures over 357°C (Fig. 2). Furthermore, several hypotheses have been suggested in the literature to explain the enhancement of C–H activation when plasma–catalyst combinations are used [23,60,61].

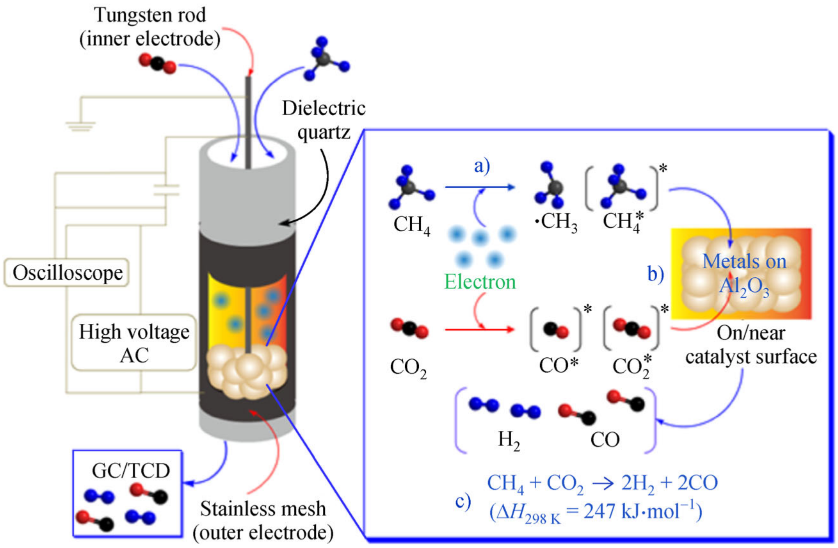

Fig. 2 Schematic representation of dry CH_4 reforming on or near the surface of an Al_2O_3-supported metal catalyst in the presence of plasma: (a) excitation of CH_4 species by gas-phase electron impact, (b) transition-metal catalyst supported on dielectric support (e.g., Al_2O_3) within plasma discharge zone, and (c) chemical equation of dry CH_4 reforming. Reprinted from ref. [59], copyright (2016), with permission from American Chemical Society

2.2 Plasma-assisted CO_2 methanation

Burning of fossil fuels increases the atmospheric CO_2 content. CO_2, which is one of the main greenhouse gases, is an extraordinarily stable molecule that absorbs infrared radiation and gives rise to global warming [62–64]. Various research groups have been working on CO_2 capture and utilization. CO_2 hydrogenation to high value-added products including hydrocarbons [65,66], methanol [67,68], formic acid [69,70], formamide [71,72], and other chemicals has been extensively studied. CO_2 methanation, which is an effective way to convert CO_2, has the advantages of a fast reaction rate, high selectivity, and fewer by-products. It is also an indispensable step in the overall process of coal gasification to produce natural gas.

$$CO_2(g) + 4H_2(g) \leftrightarrow CH_4(g) + 2H_2O(g),$$

$$\Delta H^0_{298} = -165\ \text{kJ/mol}.$$

$$CO_2(g) + H_2(g) \leftrightarrow CO(g) + H_2O(g),$$

$$\Delta H^0_{298} = 41\ \text{kJ/mol}.$$

CO_2 methanation has a small negative free energy value, which means that it can be easily performed in a wide temperature range of 27°C to 527°C (Table 1) [73]. The enthalpy value illustrates that CO_2 methanation is indeed a highly exothermic reaction. The strong heat release makes it difficult to prevent overheating and leads to inactivation of the catalyst. In some cases, the temperature becomes so high that methanation is limited by thermodynamic equilibrium. Therefore, many groups have applied a cold plasma reactor for CO_2 methanation to reduce catalyst deactivation and provide sufficient energy for this reaction.

Table 1 Thermodynamic properties of CO_2 methanation reaction

Temperature /°C	$\Delta H_f°$ /(kJ·mol^{-1})	$\Delta G°$ /(kJ·mol^{-1})	$\log K_p$
27	–165.101	–113.290	19.724
127	–170.080	–95.265	12.440
227	–174.803	–76.015	7.940
327	–179.042	–55.844	4.86
427	–182.757	–35.003	2.61
527	–185.975	–13.677	0.893
627	–188.720	+8.037	–0.466
727	–191.012	+30.012	–1.568

Plasma ionizes high-energy particles that collide with reactant molecules to activate reactive species (ions, excited molecules, atoms, free radicals, etc.). These active species interact to recombine into new species. Owing to the excellent activity of high-energy electrons in plasma, some chemical reactions are easily realized under plasma but not under conventional conditions. Chemical reactions with plasma exhibit rapid startup and fast cooling and can be implemented using simple devices. The most commonly used plasma reactors for CO_2 conversion include DBDs [74–79], microwave plasmas [80–83], nonthermal gliding arc discharges [84–87], and spark discharges [88–90].

Lee et al. [91] employed a DBD plasma reactor to investigate CO_2 methanation. The discharge frequency and H_2/CO_2 mole ratio affected the CO_2 conversion and CH_4 selectivity. Similarly, plasma–catalysis reactions are also widely studied in CO_2 methanation. For instance, Nizio et al. [92] assayed Ni-Ce-Zr hydrotalcite-derived catalysts for plasma-catalytic CO_2 methanation. High methane yields of approximately 80% were measured even at 110°C. In addition, they also used Ni-$Ce_xZr_{1-x}O_2$ with different Ce/Zr ratios to obtain 80% CO_2 conversion and 100% CH_4 selectivity in the presence of plasma at 90°C [93] (Fig. 3). The main purpose of integration of plasma and a catalyst is to obtain high energy efficiency and enhance the selectivity of the desired products. The electrical properties of the catalysts packed in the plasma are very important. Inserting different electrical catalysts into plasma reactors can cause a number of changes in the equivalent electrical circuits, which in turn affect the overall performance of the plasma reactor. Some researchers have highlighted the interaction between the plasma and catalyst [94–96], but they also faced difficulties owing to the complexity of plasma-catalytic systems. Many questions on the nature of the interactions still need to be addressed.

The reaction mechanism assists industrial amplification which occupies a crucial position in catalytic reactions. Regarding CO_2 methanation, some researchers consider that CO is an intermediate, and the process proceeds as CO methanation [97,98]. Weatherbee and Bartholomew [99] suggested a mechanism in which CO_2 was dissociatively adsorbed on active metal sites, forming adsorbed CO and O species. Subsequently, the adsorbed CO was hydrogenated to CH_4. However, others consider that carbonates/formates are intermediates and that the reaction then proceeds by hydrogenation to synthesize CH_4 [100,101]. Jiang et al. used diffuse reflectance Fourier transform infrared spectroscopy to confirm the presence of abundant oxygenates, including formate and carbonate, on the catalyst surface. Furthermore, as the amount of methane increased, the amount of oxygenates decreased [102]. However, in reactions in which plasma participates, the high-energy particles generated by plasma ionization and the molecules, radicals, and ions generated by feed gas dissociation complicate the reaction mechanism. The mechanism of the energy transfer channels and reactant interactions is not clear. According to Jwa et al. [103], CO_2 methanation occurred in three steps in a DBD plasma reactor packed with Ni/zeolite catalyst. First, dissociation of CO_2 to CO and O occurred on the active site, followed by dissociation of CO to C species and finally carbon methanation.

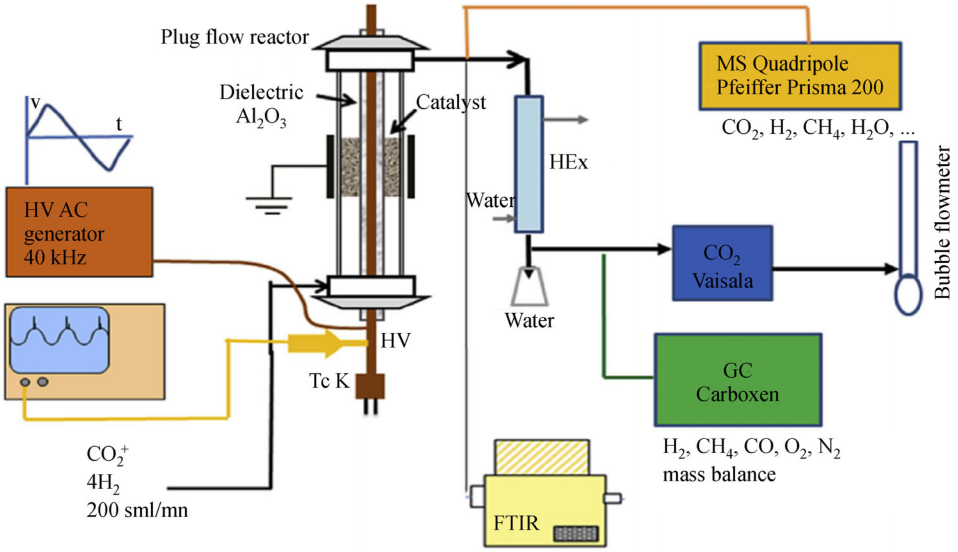

Fig. 3 Experimental setup for plasma-catalytic methanation of CO_2. Reprinted from ref. [93], copyright (2016), with permission from Elsevier

Step 1. CO_2 dissociation

$$CO_{2,ads} \leftrightarrow CO_{ads} + O_{ads};$$

Step 2. Carbon formation

$$CO_{ads} \leftrightarrow C_{ads} + O_{ads} (RDS);$$

Step 3. Carbon methanation

$$C_{ads} + H_{ads} \leftrightarrow CH_{ads},$$

$$CH_{ads} + H_{ads} \leftrightarrow CH_{2,ads},$$

$$CH_{2,ads} + 2H_{ads} \leftrightarrow CH_{4,gas}.$$

Speckmann et al. [104] controlled the water vapor by transporting oxygen ions into the reaction chamber (Fig. 4). According to their findings, H_2O and CO_2 can be used directly as precursors for methanation. The voltage applied to the ion conductor as well as the power of the plasma source current strongly affected the CO production rate. However, CH_4 production was low owing to recombination of CO and O_2 to CO_2. These results also reflect the fact that the energy efficiency (even the theoretical value) of low-pressure glow discharge plasma is lower than that of other nonthermal discharges. This remains a challenge in industrializing the low-pressure process [105]. Other researchers have also worked on the mechanism of CO_2 methanation, but no conclusion has been reached [106–108].

2.3 Plasma-assisted methane coupling reaction to C2 hydrocarbons

The methane coupling reaction is another effective way to convert natural gas to value-added products. To date, interest in catalyst preparation, basic research, and reaction processes has resulted in dozens of papers and patents [109,110]. As mentioned above, methane is one of the most stable molecules, so a large amount of energy is required for its conversion to higher hydrocarbons. A high-temperature reaction induces deactivation of the catalyst and a decrease in the C2 hydrocarbon yield. Accordingly, the use of cold plasmas in this reaction is very important to improve the productivity of C2 hydrocarbons and prolong the catalyst life. Lee et al. [111] compared several plasma reactors used for methane conversion; their findings are summarized in Table 2. The results suggest that the product distribution can be controlled by varying the degree of warmth of the plasma source.

Zhang et al. [112] employed a Pd catalyst doped with the ionic liquid l-hexyl-3-methylimidazolium tetrafluoroborate (C_6MIMBF_4) for the methane coupling reaction (Fig. 5). They inferred that in a cold plasma reactor, elastic collision of methane with energized electrons may produce radicals such as CH_3•, CH_2•, and CH•. Moreover, C_6MIMBF_4 is a weak Brönsted acid that can efficiently attract these radicals to accelerate their combination, thus promoting the selectivity of C2 hydrocarbons [113].

Nozaki et al. conducted a similar study [114]. Considering electronic collision, several reaction paths for the formation of C_2H_2 and alkenes are provided below [111]. The production of C_2H_2, C_2H_4, and C_3H_6 depends on the concentration of alkanes such as C_2H_6 and C_3H_8.

$$e + C_2H_6 \rightarrow e + C_2H_4 + H_2$$

$$e + C_2H_4 \rightarrow e + C_2H_2 + H_2$$

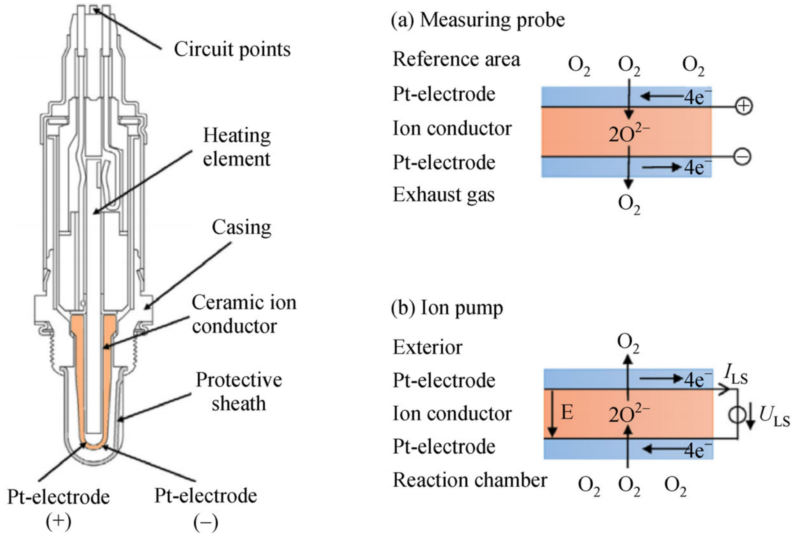

Fig. 4 Components of a switching-TPE lambda probe and bidirectional ion transport through the ceramic (yttria-stabilized zirconia) ion conductor. Reprinted from ref. [104], copyright (2017), with permission from Elsevier

Table 2 Product analysis of methane coupling reaction in different plasma sources. Reprinted from ref. [111], copyright (2013), with permission from Springer

Material	Molar ratio /%						
	AC DBD	Pulsed DBD	Pulsed Spark	AC Spark	Hollow Cathode	Gliding Arc	Rotating Arc
H_2	0.520	0.210	1.373	2.920	0.850	1.83	1.310
C_2H_6	0.106	0.065	0.026	0.000	0.014	–	0.002
C_2H_4	0.007	0.003	0.031	0.024	0.015	–	0.011
C_3H_8	0.018	0.009	0.002	0.000	0.000	–	0.000
C_3H_6	0.002	0.000	0.005	0.000	0.003	–	0.000
C_2H_2	0.008	0.003	0.459	0.860	0.270	0.272	0.420
CH_4 conv. /%	14.76	12.375	49.405	82.930	25.772	23.72	42.170
Sel.(H_2) /%	36.457	19.312	32.249	42.053	33.173	73.2	34.815
Sel.(C_2H_2) /%	2.243	1.104	43.124	49.171	42.149	43.52	44.649

$$e + C_3H_8 \rightarrow e + C_3H_6 + H_2$$

$$e + C_3H_6 \rightarrow e + C_2H_2 + CH_4$$

The energy density (E_d) and energy efficiency (η_E) are two important parameters in a plasma reaction [115]. In a glow plasma reactor, the catalytic activity of the methane coupling reaction to C2 hydrocarbons has a linear relationship with the energy density, as shown in Fig. 6. In a certain range, increasing E_d facilitates the interaction between methane and high-energy electrons, enhancing the methane conversion and C2 hydrocarbon yield. Nevertheless, when E_d is too large, further breakage of C–H bonds will occur, forming carbon deposits and reducing the C2 hydrocarbon yield. Other papers also suggested this linearity with respect to increasing input power [116–120]. As shown in Fig. 7, this linear relationship between the energy density and energy efficiency is quite different from their relationship with respect to the catalytic activity. With an increase in energy density, the energy efficiency of the reaction gradually decreases.

The following matters associated with the plasma-assisted methane coupling reaction still need to be addressed: (1) the mechanism of the plasma-assisted reaction process, including the interaction between substances in the gas with the plasma and mutual collision of the substances in a plasma environment, and (2) the development of high-activity discharge plasma generation technology, which is related to the reaction rate and energy utilization efficiency of the plasma-catalytic reaction.

3 Plasma-assisted VOC abatement

“VOC” is a general term for volatile organic compounds with a melting point below room temperature and a boiling

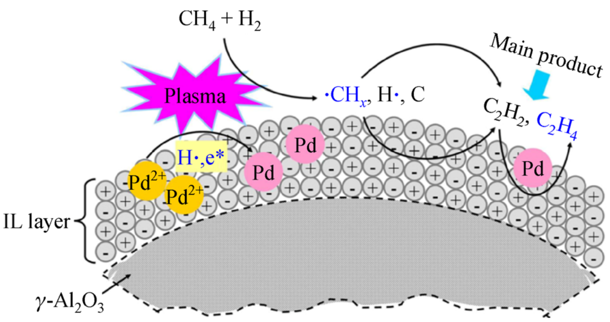

Fig. 5 Schematic illustration of methane conversion under plasma over Pd-IL/γ-Al_2O_3. Reprinted from ref. [112], copyright (2013), with permission from Elsevier

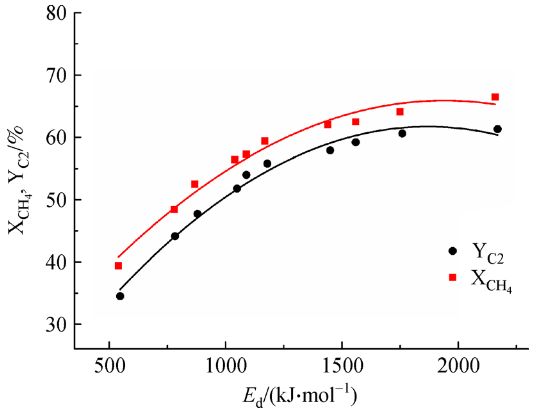

Fig. 6 Effect of energy density on CH_4 conversion and C2 hydrocarbon yield. Reprinted from ref. [115], copyright (2006), with permission from Nuclear Fusion and Plasma Physics

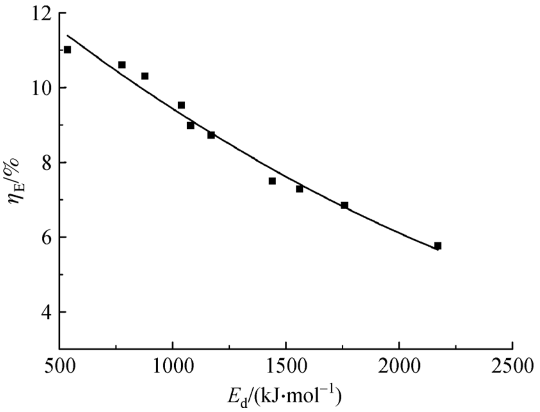

Fig. 7 Energy efficiency of CH_4 coupling reaction. Reprinted from ref. [115], copyright (2006), with permission from Nuclear Fusion and Plasma Physics

point between 50°C and 260°C. They pose a serious threat to human health and the environment. Many techniques for removing VOCs are costly and difficult to apply, in contrast to NTP approaches [121–124]. When the concentration of VOCs is low (up to 1000 ppm), complete removal by conventional methods is difficult. Unfortunately, the poor product selectivity, formation of undesired by-products, and low energy efficiency are three main obstacles that impede the industrialization of plasma approaches. To overcome these problems, a series of hybrid system such as NTP/electrostatic precipitation [125], packed-bed NTP reactors [126], and adsorption/NTP [127], NTP/catalysis [128,129], and photocatalysis [130] techniques have been established.

The simple packed-bed plasma reactors reported thus far, however, have many drawbacks for effective decomposition of VOCs, including low energy efficiencies, poor selectivity to CO_2 in the reaction products, and by-product formation [131,132]. In 1999, Ogata et al. introduced alumina into the plasma reactor as an adsorption material. The results indicated better benzene decomposition efficiency compared to that of plasma alone without alumina [133]. Soon after, they tried zeolite, which showed a 1.4–2.1 times higher benzene decomposition efficiency [134] (Fig. 8). Oh et al. [135] also confirmed accelerated oxidation of toluene in a plasma reactor when a zeolite adsorbent was used. Subsequently, plasma hybrid systems became a topic of research. Kuroki et al. [136] developed a gas circulation system in which ozone was circulated to oxidize toluene (Fig. 9). This system realized high toluene conversion with no ozone waste.

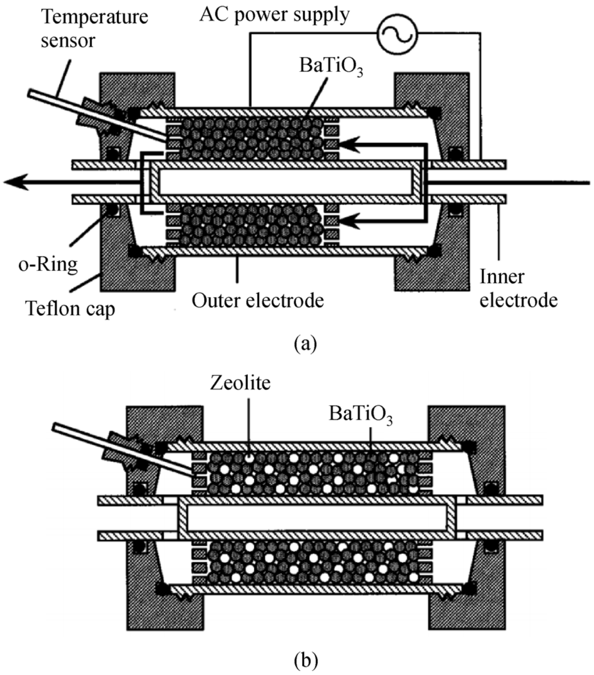

Fig. 8 Reactor configurations: (a) conventional reactor, (b) zeolite-hybrid reactor. Reprinted from ref. [134], copyright (2001), with permission from IEEE

Feng et al. [137] designed a three-stage plasma-assisted catalysis system consisting of a DBD stage, back-corona discharge (BCD) stage, and catalyst stage to drastically reduce the pressure drop in the catalyst layer (Fig. 10). They successfully achieved a high removal efficiency of almost 100%.

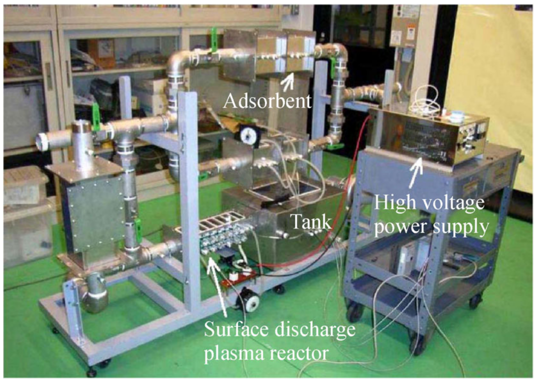

Fig. 9 Overview of equipment for toluene oxidation in a gas circulation system. Reprinted from ref. [136], copyright (2011), with permission from IEEE

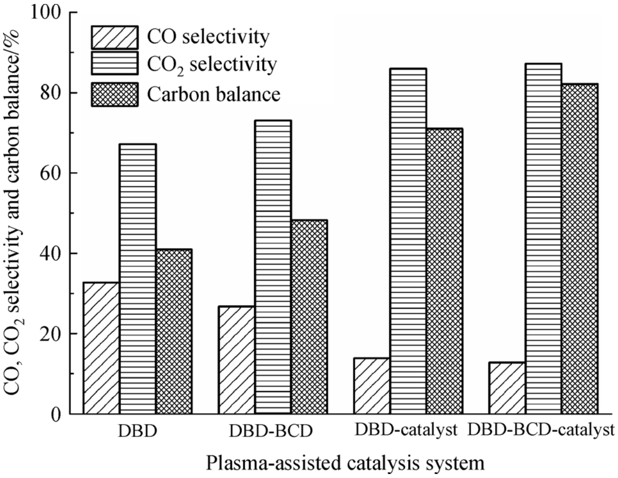

Fig. 10 CO selectivity, CO_2 selectivity, and carbon balance of the three-stage system in four different conditions: DBD alone, DBD-BCD, DBD-catalyst, and DBD-BCD-catalyst. The specific input energy of DBD and BCD is fixed at 64 and 128.9 J/L, respectively. Reprinted from ref. [137], copyright (2015), with permission from American Chemical Society

Many other researchers have also reported on the application of plasma for VOC abatement. Sultana et al. [138] thoroughly summarized the articles concerning sequential plasma treatment for VOC abatement and the current status of this new technique. Schiavon et al. [139] described in detail the types of plasma and parameters for VOC treatment. Vandenbroucke et al. [140] focused on plasma-alone and plasma-catalytic treatment for VOC abatement. Feng et al. [141] studied the synergistic effects and mechanism of an NTP-catalysis system for VOC removal. Current plasma (catalytic) technology has not been able to completely eliminate VOCs and their organic intermediates by the oxidation reaction owing to the complex molecular structure of the organic compounds. Further, aerosol generation remains a problem. Therefore, the design of new high-energy plasma sources and new catalysts for coupling with plasma light, heat, electron, and other effects are potential solutions for degradation of VOCs.

4 Plasma for treatment of metal–organic frameworks

The use of plasma in catalyst calcination, reduction, and modification has been comprehensively studied [18,142, 143]. Note that the option of room-temperature operation of plasma makes it an excellent candidate for thermally sensitive materials, such as porous organic materials, peptides, proteins, conducting polymers, and ultrahigh-surface-area carbon [144–147].

MOFs, a new family of crystalline porous materials, have found applications in many fields, such as gas storage and separation, chemical sensing, drug delivery, luminescence, ion exchange, and heterogeneous catalysis [148,149]. They not only combine the beneficial characteristics of inorganic and organic components but also frequently show unique properties that exceed those expected of a simple mixture of the components. However, the thermal instability of MOFs limits their application in catalytic reactions. According to thermogravimetric analysis, ZIF-67 begins to disassemble at approximately 500°C in nitrogen, Co-MOF-74 degradation begins at approximately 450°C in nitrogen, and ZIF-8 degradation begins at approximately 550°C in nitrogen. Data for these and other MOFs are shown in Table 3.

Table 3 Thermogravimetric analysis of various MOFs

Catalyst	Temperature /°C	Ref.
ZIF-67	500	148
ZIF-8	550	149
Co-MOF-74	450	150
Ni-MOF-74	300	151
MIL-101	330	152
MOF-5	400	153
Cu-BTC	280	154
UiO-66	500	155

Accordingly, researchers have attempted to apply cold plasma to this material and maintain its original skeleton structure. Sadakiyo et al. [156] applied the arc plasma deposition (APD) method to prepare MOF-supported metal nanoparticles, as illustrated schematically in Fig. 11. Various transition metal nanoparticles such as Pt, Pd, and Ru on different types of MOF composed of ZIF-8 [157], MIL-101 [158], UiO-66-NH_2 [159], and Zn-MOF-74 [160] have been reported. The results revealed that the metal particles deposited on the MOF supports had similar sizes, with a diameter of approximately 2 nm.

Bahri et al. [161] used MIL-101, MIL-53, and CPM-5 in

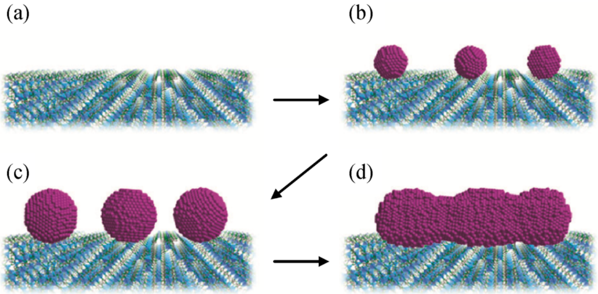

Fig. 11 Schematic of particle formation process on MOFs: (a) Blank MOFs; (b) Formation of seed particles (approximately 1 nm in diameter) at low metal loadings (for Pt ≈ 0.5 wt.% metal loading) by APD irradiation; (c) Particle growth up to approximately 2 nm in diameter by further APD irradiation (0.5 wt.% –1.5 wt.%); (d) Formation of nanorods by further APD irradiation (above 2 wt.%). Reprinted from ref. [156], copyright (1996), with permission from Royal Society of Chemistry

an NTP-catalytic reactor to remove 1 ppm toluene and isobutanol. All three MOFs exhibited high removal efficiencies of 100% for isobutanol and approximately 90% for toluene in dry air. Li et al. [162] carbonized MIL-100 and MIL-10 onto synthesized Al_2O_3 and Cr_2O_3 nanoparticles. Use of O_2 plasma was required to obtain high-quality crystalline metal oxides. Analogously, Dou et al. [163] realized on-site formation of atomic-scale CoO_x species from ZIF-67 by O_2 plasma. The obtained CoO_x catalyst with atomic-scale active sites exhibited excellent performance (even better than that of the RuO_2 catalyst) for the oxygen evolution reaction.

5 Conclusions

In this paper, we summarized the applications of plasma in various reactions: dry reforming of methane, carbon dioxide methanation, the methane coupling reaction to C2 hydrocarbons, and VOC abatement. Both plasma-alone and plasma catalysis techniques have drawn considerable attention. The catalytic performance is affected not only by the properties of the catalysts but also by the plasma configuration. Various configurable plasmas and different types of catalysts have been tested. Under optimized plasma parameters and reaction conditions, the catalytic activity has been improved to varying extents with or without catalysts. Although many researchers have devoted considerable effort to elucidating the reaction mechanisms under plasma, our knowledge of these mechanisms is still insufficient. In addition, plasma also provides a new treatment method for MOFs and other heat-sensitive materials. As stated above, plasma, with its excellent properties, shows great promise for use in these reactions. We hope that on the basis of existing accomplishments, further progress can be made in future.

References

1. Mott-Smith H M. History of “plasmas”. Nature, 1971, 233(5316): 219–219
2. Jiang B, Zheng J T, Qiu S, Wu M B, Zhang Q H, Yan Z F, Xue Q Z. Review on electrical discharge plasma technology for wastewater remediation. Chemical Engineering Journal, 2014, 236: 348–368
3. Hinokuma S, Misumi S, Yoshida H, Machida M. Nanoparticle catalyst preparation using pulsed arc plasma deposition. Catalysis Science & Technology, 2015, 5(9): 4249–4257
4. Samukawa S, Hori M, Rauf S, Tachibana K, Bruggeman P, Kreesen G, Whitehead I C, Murphy A B, Gutsol A F, Starikovskaia S. The 2012 plasma roadmap. Journal of Physics. D, Applied Physics, 2012, 45(25): 253001
5. Kim S H, Moon S Y, Park J Y. Non-colloidal nanocatalysts fabricated using arc plasma deposition and their application in heterogenous catalysis and photocatalysis. Topics in Catalysis, 2017, 60(12): 812–822
6. Liu C J, Vissokov G P, Jang B W L. Catalyst preparation using plasma technologies. Catalysis Today, 2002, 72(3-4): 173–184
7. Wang Z Y, Liu C J. Preparation and application of iron oxide/graphene based composites for electrochemical energy storage and energy conversion devices: Current status and perspective. Nano Energy, 2015, 11: 277–293
8. Liu C J, Li M Y, Wang J Q, Zhou X T, Guo Q T, Yan J M, Li Y Z. Plasma methods for preparing green catalysts: Current status and perspective. Chinese Journal of Catalysis, 2016, 37(3): 340–348
9. Li H Q, Zou J J, Liu C J. Progress in hydrogen generation using plasmas. Progress in Chemistry, 2005, 17(1): 69–77
10. Bian L, Zhang L, Xia R, Li Z H. Enhanced low-temperature CO_2 methanation activity on plasma-prepared Ni-based catalyst. Journal of Natural Gas Science and Engineering, 2015, 27: 1189–1194
11. Fu T J, Huang C D, Lv J, Li Z H. Fischer-Tropsch performance of an SiO_2-supported Co-based catalyst prepared by hydrogen dielectric-barrier discharge plasma. Plasma Science & Technology, 2014, 16(3): 232–238
12. Park S, Choe W, Moon S Y, Yoo S J. Electron characterization in weakly ionized collisional plasmas: From principles to techniques. Advances in Physics-X, 2018, 4(1): 1526114
13. Ouyang J, Li B, He F, Dai D. Nonlinear phenomena in dielectric barrier discharges: Pattern, striation and chaos. Plasma Science & Technology, 2018, 20(10): 103002
14. Borra J P. Review on water electro-sprays and applications of charged drops with focus on the corona-assisted cone-jet mode for high efficiency air filtration by wet electro-scrubbing of aerosols. Journal of Aerosol Science, 2018, 125: 208–236
15. Yi H H, Zhao S Z, Tang X L, Song C Y, Gao F Y, Zhang B W, Wang Z X, Zuo Y R. Low-temperature hydrolysis of carbon disulfide using the Fe-Cu/AC catalyst modified by non-thermal plasma. Fuel, 2014, 128: 268–273
16. Naseh M V, Khodadadi A A, Mortazavi Y, Pourfayaz F, Alizadeh O, Maghrebi M. Fast and clean functionalization of carbon nanotubes by dielectric barrier discharge plasma in air compared to

acid treatment. Carbon, 2010, 48(5): 1369–1379

17. Chen Q, Kaneko T, Hatakeyama R. Rapid synthesis of water-soluble gold nanoparticles with control of size and assembly using gas-liquid interfacial discharge plasma. Chemical Physics Letters, 2012, 521: 113–117
18. Zhou C M, Chen H, Yan Y B, Jia X L, Liu C J, Yang Y H. Argon plasma reduced Pt nanocatalysts supported on carbon nanotube for aqueous phase benzyl alcohol oxidation. Catalysis Today, 2013, 211: 104–108
19. Liu C J, Zhao Y, Li Y Z, Zhang D S, Chang Z, Bu X H. Perspectives on electron-assisted reduction for preparation of highly dispersed noble metal catalysts. ACS Sustainable Chemistry & Engineering, 2014, 2(1): 3–13
20. Ohkubo Y, Hamaguchi Y, Seino S, Nakagawa T, Kageyama S, Kugai J, Nitani H, Ueno K, Yamamoto T A. Preparation of carbon-supported PtCo nanoparticle catalysts for the oxygen reduction reaction in polymer electrolyte fuel cells by an electron-beam irradiation reduction method. Journal of Materials Science, 2013, 48(14): 5047–5054
21. Pastor-Perez L, Belda-Alcazar V, Marini C, Pastor-Blas M M, Sepulveda-Escribana A, Ramos-Fernandez E V. Effect of cold Ar plasma treatment on the catalytic performance of Pt/CeO_2 in water-gas shift reaction (WGS). Applied Catalysis B: Environmental, 2018, 225: 121–127
22. Liu C, Lan J P, Sun F L, Zhang Y H, Li J L, Hong J P. Promotion effects of plasma treatment on silica supports and catalyst precursors for cobalt Fischer-Tropsch catalysts. RSC Advances, 2016, 6(62): S7701–S7708
23. Neyts E C, Ostrikov K, Sunkara M K, Bogaerts A. Plasma catalysis: Synergistic effects at the nanoscale. Chemical Reviews, 2015, 115(24): 13408–13446
24. Wang Z, Zhang Y, Neyts E C, Cao X X, Zhang X S, Jang B W L, Liu C J. Catalyst preparation with plasmas: How does it work? ACS Catalysis, 2018, 8(3): 2093–2110
25. Sadakiyo M, Heima M, Yamamoto T, Matsumura S, Matsuura M, Sugimoto S, Kato K, Takata M, Yamauchi M. Preparation of solid-solution type Fe-Co nanoalloys by synchronous deposition of Fe and Co using dual arc plasma guns. Dalton Transactions (Cambridge, England), 2015, 44(36): 15764–15768
26. Rosi N L, Kim J, Eddaoudi M, Chen B L, O'Keeffe M, Yaghi O M. Rod packings and metal-organic frameworks constructed from rod-shaped secondary building units. Journal of the American Chemical Society, 2005, 127(5): 1504–1518
27. Gilman A B, Piskarev M S, Kuznetsov A A, Ozerin A N. Modification of ultrahigh-molecular-weight polyethylene by low-temperature plasma. High Energy Chemistry, 2017, 51(2): 136–144
28. Sun Y P, Nie Y, Yuan J, Wu A S, Shen J L, Ji D X, Yu F W, Ji J B. Application of plasma technology in the reaction of methane carbon dioxide reforming to syngas. Chemical Industry and Engineering Progress, 2010, 29(S1): 295–300
29. Chung W C, Chang M B. Review of catalysis and plasma performance on dry reforming of CH_4 and possible synergistic effects. Renewable & Sustainable Energy Reviews, 2016, 62: 13–31
30. Zhou T, Jang K, Jang B W L. Ionic liquid and plasma effects on SiO_2 supported Pd for selective hydrogenation of acetylene. Catalysis Today, 2013, 211: 147–155
31. Zhou C M, Wang X, Jia X L, Wang H P, Liu C J, Yang Y H. Nanoporous platinum grown on nickel foam by facile plasma reduction with enhanced electro-catalytic performance. Electrochemistry Communications, 2012, 18: 33–36
32. Platonov E A, Bratchikova I G, Yagodovskii V D, Murga Z V. Carbon dioxide reforming of methane on a cobalt catalyst subjected to plasma-chemical treatment. Russian Journal of Physical Chemistry A, 2017, 91(8): 1422–1426
33. Wu Y W, Chung W C, Chang M B. Modification of Ni/gamma-Al_2O_3 catalyst with plasma for steam reforming of ethanol to generate hydrogen. International Journal of Hydrogen Energy, 2015, 40(25): 8071–8080
34. Zhu B, Jang B W L. Insights into surface properties of non-thermal RF plasmas treated Pd/TiO_2 in acetylene hydrogenation. Journal of Molecular Catalysis A Chemical, 2014, 395: 137–144
35. Movasati A, Alavi S M, Mazloom G. Dry reforming of methane over CeO_2-$ZnAl_2O_4$ supported Ni and Ni-Co nano-catalysts. Fuel, 2019, 236: 1254–1262
36. Song K, Lu M, Xu S, Chen C, Zhan Y, Li D, Au C, Jiang L, Tomishige K. Effect of alloy composition on catalytic performance and coke-resistance property of Ni-Cu/Mg(Al)O catalysts for dry reforming of methane. Applied Catalysis B: Environmental, 2018, 239: 324–333
37. Li Z, Das S, Hongmanorom P, Dewangan N, Wai M H, Kawi S. Silica-based micro- and mesoporous catalysts for dry reforming of methane. Catalysis Science & Technology, 2018, 8(11): 2763–2778
38. Tu X, Whitehead J C. Plasma dry reforming of methane in an atmospheric pressure AC gliding arc discharge: Co-generation of syngas and carbon nanomaterials. International Journal of Hydrogen Energy, 2014, 39(18): 9658–9669
39. Lim M S, Chun Y N. Carbon dioxide destruction with methane reforming by a novel plasma-catalytic converter. Plasma Chemistry and Plasma Processing, 2016, 36(5): 1211–1228
40. Li X S, Zhu B, Shi C, Xu Y, Zhu A M. Carbon dioxide reforming of methane in kilohertz spark-discharge plasma at atmospheric pressure. AIChE Journal. American Institute of Chemical Engineers, 2011, 57(10): 2854–2860
41. Zhou Z P, Zhang J M, Ye T H, Zhao P H, Xia W D. Hydrogen production by reforming methane in a corona inducing dielectric barrier discharge and catalyst hybrid reactor. Chinese Science Bulletin, 2011, 56(20): 2162–2166
42. Li X, Tao X M, Yin Y X. An atmospheric-pressure glow-discharge plasma jet and its application. IEEE Transactions on Plasma Science, 2009, 37(6): 759–763
43. Jo S, Lee D H, Song Y H. Product analysis of methane activation using noble gases in a non-thermal plasma. Chemical Engineering Science, 2015, 130: 101–108
44. Park S, Lee M, Bae J, Hong D Y, Park Y K, Hwang Y K, Jeong M G, Kim Y D. Plasma-assisted non-oxidative conversion of methane over Mo/HZSM-5 catalyst in DBD reactor. Topics in Catalysis, 2017, 60(9-11): 735–742
45. Ray D, Reddy P M K, Challapalli S. Glass beads packed DBD-plasma assisted dry reforming of methane. Topics in Catalysis,

2017, 60(12-14): 869–878

46. Zhang K, Mukhriza T, Liu X T, Greco P P, Chiremba E. A study on CO_2 and CH_4 conversion to synthesis gas and higher hydrocarbons by the combination of catalysts and dielectric-barrier discharges. Applied Catalysis A, General, 2015, 502: 138–149
47. Zheng X G, Tan S Y, Dong L C, Li S B, Chen H M, Wei S A. Experimental and kinetic investigation of the plasma catalytic dry reforming of methane over perovskite $LaNiO_3$ nanoparticles. Fuel Processing Technology, 2015, 137: 250–258
48. Chung W C, Tsao I Y, Chang M B. Novel plasma photocatalysis process for syngas generation via dry reforming of methane. Energy Conversion and Management, 2018, 164: 417–428
49. Xia Y, Lu N, Wang B, Li J, Shang K, Jiang N, Wu Y. Dry reforming of CO_2-CH_4 assisted by high-frequency AC gliding arc discharge: Electrical characteristics and the effects of different parameters. International Journal of Hydrogen Energy, 2017, 42 (36): 22776–22785
50. Montoro-Damas A M, Brey J J, Rodríguez M A, Gonzalez-Elipe A R, Cotrino J. Plasma reforming of methane in a tunable ferroelectric packed-bed dielectric barrier discharge reactor. Journal of Power Sources, 2015, 296: 268–275
51. Jin L J, Li Y, Feng Y Q, Hu H Q, Nu A M. Integrated process of coal pyrolysis with CO_2 reforming of methane by spark discharge plasma. Journal of Analytical and Applied Pyrolysis, 2017, 126: 194–200
52. Mustafa M F, Fu X D, Lu W J, Liu Y J, Abbas Y, Wang H T, Arslan M T. Application of non-thermal plasma technology on fugitive methane destruction: Configuration and optimization of double dielectric barrier discharge reactor. Journal of Cleaner Production, 2018, 174: 670–677
53. Nguyen H H, Nasonova A, Nah I W, Kim K S. Analysis on CO_2 reforming of CH_4 by corona discharge process for various process variables. Journal of Industrial and Engineering Chemistry, 2015, 32: 58–62
54. Wang B W, Sun Q M, Lu Y J, Yang M L, Yan W J. Steam reforming of dimethyl ether by gliding arc gas discharge plasma for hydrogen production. Chinese Journal of Chemical Engineering, 2014, 22(1): 104–112
55. Iwarere S A, Rohani V J, Ramjugernath D, Fulcheri L. Dry reforming of methane in a tip-tip arc discharge reactor at very high pressure. International Journal of Hydrogen Energy, 2015, 40(8): 3388–3401
56. Xu G H, Jiang E Y, Sheng J. Technology and application of plasma. Beijing: Chemical Industry Press, 2006: 1–242 (in Chinese)
57. Yap D, Tatibouet J M, Batiot-Dupeyrat C. Catalyst assisted by non-thermal plasma in dry reforming of methane at low temperature. Catalysis Today, 2018, 299: 263–271
58. Sentek J, Krawczyk K, Mlotek M, Kalczewska M, Kroker T, Kolb T, Schenk A, Gericke K H, Schmidt-Szalowski K. Plasma-catalytic methane conversion with carbon dioxide in dielectric barrier discharges. Applied Catalysis B: Environmental, 2010, 94(1-2): 19–26
59. Kim J, Abbott M S, Go D B, Hicks J C. Enhancing C–H bond activation of methane via temperature-controlled, catalyst-plasma interactions. ACS Energy Letters, 2016, 1(1): 94–99
60. Snoeckx R, Aerts R, Tu X, Bogaerts A. Plasma-based dry reforming: A computational study ranging from the nanoseconds to seconds time scale. Journal of Physical Chemistry C, 2013, 117 (10): 4957–4970
61. Kim H H, Teramoto Y, Negishi N, Ogata A. A multidisciplinary approach to understand the interactions of nonthermal plasma and catalyst: A review. Catalysis Today, 2015, 256: 13–22
62. Meinshausen M, Meinshausen N, Hare W, Raper S C B, Frieler K, Knutti R, Frame D J, Allen M R. Greenhouse-gas emission targets for limiting global warming to 2°C. Nature, 2009, 458(7242): 1158–1162
63. Matthews H D, Gillett N P, Stott P A, Zickfeld K. The proportionality of global warming to cumulative carbon emissions. Nature, 2009, 459(7248): 829–832
64. Wise M, Calvin K, Thomson A, Clarke L, Bond-Lamberty B, Sands R, Smith S J, Janetos A, Edmonds J. Implications of limiting CO_2 concentrations for land use and energy. Science, 2009, 324 (5931): 1183–1186
65. Lu Y W, Yan Q G, Han J, Cao B B, Street J, Yu F. Fischer-Tropsch synthesis of olefin-rich liquid hydrocarbons from biomass-derived syngas over carbon-encapsulated iron carbide/iron nanoparticles catalyst. Fuel, 2017, 193: 369–384
66. Foit S R, Vinke I C, de Haart L G J, Eichel R A. Power-to-syngas: An enabling technology for the transition of the energy system? Angewandte Chemie International Edition, 2017, 56(20): 5402–5411
67. Wang L, Yi Y H, Guo H C, Tu X. Atmospheric pressure and room temperature synthesis of methanol through plasma-catalytic hydrogenation of CO_2. ACS Catalysis, 2018, 8(1): 90–100
68. Saeidi S, Amin N A S, Rahimpour M R. Hydrogenation of CO_2 to value-added products—A review and potential future developments. Journal of CO_2 Utilization, 2014, 5: 66–81
69. Federsel C, Jackstell R, Beller M. State-of-the-art catalysts for hydrogenation of carbon dioxide. Angewandte Chemie International Edition, 2010, 49(36): 6254–6257
70. Dimitriou I, Garcia-Gutierrez P, Elder R H, Cuellar-France R M, Azapagic A, Allen R W K. Carbon dioxide utilisation for production of transport fuels: Process and economic analysis. Energy & Environmental Science, 2015, 8(6): 1775–1789
71. Omae I. Aspects of carbon dioxide utilization. Catalysis Today, 2006, 115(1): 33–52
72. Jessop P G, Ikariya T, Noyori R. Homogeneous catalytic-hydrogen of carbon dioxide. Nature, 1994, 368(6468): 231–233
73. Alexmills G, Steffgen F. Catalytic methanation. Catalysis Reviews, 1974, 8(1): 159–210
74. Paulussen S, Verheyde B, Tu X, De Bie C, Martens T, Petrovic D, Bogaerts A, Sels B. Conversion of carbon dioxide to value-added chemicals in atmospheric pressure dielectric barrier discharges. Plasma Sources Science & Technology, 2010, 19(3): 34015–34016
75. Pinhão N R, Janeco A, Branco J B. Influence of helium on the conversion of methane and carbon dioxide in a dielectric barrier discharge. Plasma Chemistry and Plasma Processing, 2011, 31(3): 427–439
76. Eliasson B, Kogelschatz U, Xue B Z, Zhou L M. Hydrogenation of carbon dioxide to methanol with a discharge-activated catalyst. Industrial & Engineering Chemistry Research, 1998, 37(8): 3350–

3357

77. Gómez-Ramírez A, Rico V J, Cotrino J, Gonzalez-Elipe A, Lambert R M. Low temperature production of formaldehyde from carbon dioxide and ethane by plasma-assisted catalysis in a ferroelectrically moderated dielectric barrier discharge reactor. ACS Catalysis, 2014, 4(2): 402–408
78. Van Laer K, Bogaerts A. Improving the conversion and energy efficiency of carbon dioxide splitting in a zirconia-packed dielectric barrier discharge reactor. Energy Technology (Weinheim), 2015, 3(10): 1038–1044
79. Ramakers M, Michielsen I, Aerts R, Meynen V, Bogaerts A. Effect of argon or helium on the CO_2 conversion in a dielectric barrier discharge. Plasma Processes and Polymers, 2015, 12(8): 755–763
80. van Rooij G J, van den Bekerom D C M, den Harder N, Minea T, Berden G, Bongers W A, Engeln R, Graswinckel M F, Zoethout E, de Sandena M C M V. Taming microwave plasma to beat thermodynamics in CO_2 dissociation. Faraday Discussions, 2015, 183: 233–248
81. Bongers W, Bouwmeester H, Wolf B, Peeters F, Welzel S, van den Bekerom D, den Harder N, Goede A, Graswinckel M, Green P W, et al. Plasma-driven dissociation of CO_2 for fuel synthesis. Plasma Processes and Polymers, 2017, 14(6): 1600126
82. Silva T, Britun N, Godfroid T, Snyders R. Optical characterization of a microwave pulsed discharge used for dissociation of CO_2. Plasma Sources Science & Technology, 2014, 23(2): 217–221
83. Spencer L F, Gallimore A D. CO_2 dissociation in an atmospheric pressure plasma/catalyst system: A study of efficiency. Plasma Sources Science & Technology, 2013, 22(1): 015019
84. Ramakers M, Trenchev G, Heijkers S, Wang W Z, Bogaerts A. Gliding arc plasmatron: Providing an alternative method for carbon dioxide conversion. ChemSusChem, 2017, 10(12): 2642–2652
85. Li K, Liu J L, Li X S, Zhu X B, Zhu A M. Warm plasma catalytic reforming of biogas in a heat-insulated reactor: Dramatic energy efficiency and catalyst auto-reduction. Chemical Engineering Journal, 2016, 288: 671–679
86. Liu J L, Park H W, Chung W J, Ahn W S, Park D W. Simulated biogas oxidative reforming in AC-pulsed gliding arc discharge. Chemical Engineering Journal, 2016, 285: 243–251
87. Liu J L, Park H W, Chung W J, Park D W. High-efficient conversion of CO_2 in AC-pulsed tornado gliding arc plasma. Plasma Chemistry and Plasma Processing, 2016, 36(2): 437–449
88. Shapoval V, Marotta E, Ceretta C, Konjevic N, Ivkovic M, Schiorlin M, Paradisi C. Development and testing of a self-triggered spark reactor for plasma driven dry reforming of methane. Plasma Processes and Polymers, 2014, 11(8): 787–797
89. Zhu B, Li X S, Shi C, Liu J L, Zhao T L, Zhu A M. Pressurization effect on dry reforming of biogas in kilohertz spark-discharge plasma. International Journal of Hydrogen Energy, 2012, 37(6): 4945–4954
90. Zhu B, Li X S, Liu J L, Zhu X B, Zhu A M. Kinetics study on carbon dioxide reforming of methane in kilohertz spark-discharge plasma. Chemical Engineering Journal, 2015, 264: 445–452
91. Lee C J, Lee D H, Kim T. Enhancement of methanation of carbon dioxide using dielectric barrier discharge on a ruthenium catalyst at atmospheric conditions. Catalysis Today, 2017, 293: 97–104
92. Nizio M, Benrabbah R, Krzak M, Debek R, Motak M, Caavadias S, Galvez M E, Da Costa P. Low temperature hybrid plasma-catalytic methanation over Ni-Ce-Zr hydrotalcite-derived catalysts. Catalysis Communications, 2016, 83: 14–17
93. Nizio M, Albarazi A, Cavadias S, Amouroux J, Galvez M E, Da Costa P. Hybrid plasma-catalytic methanation of CO_2 at low temperature over ceria zirconia supported Ni catalysts. International Journal of Hydrogen Energy, 2016, 41(27): 11584–11592
94. Zhang Y R, Van Laer K, Neyts E C, Bogaerts A. Can plasma be formed in catalyst pores? A modeling investigation. Applied Catalysis B: Environmental, 2016, 185: 56–67
95. Bruggeman P J, Kushner M J, Locke B R, Gardeniers J G E, Graham W G, Graves D B, Hofmann-Caris R C H M, Maric D, Reid J P, Ceriani E, et al. Plasma-liquid interactions: A review and roadmap. Plasma Sources Science & Technology, 2016, 25(5): 1–125
96. Bruggeman P J, Czarnetzki U. Retrospective on ‘The 2012 Plasma Roadmap’. Journal of Physics. D, Applied Physics, 2016, 49(43): 431001
97. Aziz M A A, Jalil A A, Triwahyono S, Mukti R R, Taufiq-Yap Y H, Sazegar M R. Highly active Ni-promoted mesostructured silica nanoparticles for CO_2 methanation. Applied Catalysis B: Environmental, 2014, 147: 359–368
98. Ren J, Guo H L, Yang J Y, Qin Z F, Lin J Y, Li Z. Insights into the mechanisms of CO_2 methanation on Ni(111) surfaces by density functional theory. Applied Surface Science, 2015, 351: 504–516
99. Weatherbee G D, Bartholomew C H. Hydrogenation of CO_2 on group VIII metals. II. Kinetics and mechanism of CO_2 hydrogenation on nickel. Journal of Catalysis, 1982, 77(2): 460–472
100. Upham D C, Derk A R, Sharma S, Metiu H, McFarland E W. CO_2 methanation by Ru-doped ceria: The role of the oxidation state of the surface. Catalysis Science & Technology, 2015, 5(3): 1783–1791
101. Azzolina-Jury F, Bento D, Henriques C, Thibault-Starzyk F. Chemical engineering aspects of plasma-assisted CO_2 hydrogenation over nickel zeolites under partial vacuum. Journal of CO_2 Utilization, 2017, 22: 97–109
102. Jiang Q, Lin Q, Huang Z T. Study on carbon dioxide methanation catalyst III. Catalytic reaction mechanism under the action of Ni-Ru- rare earth/ZrO_2. Journal of Catalysis, 1997, (3): 189–139 (in Chinese)
103. Jwa E, Lee S B, Lee H W, Mok Y S. Plasma-assisted catalytic methanation of CO and CO_2 over Ni-zeolite catalysts. Fuel Processing Technology, 2013, 108: 89–93
104. Speckmann F W, Mueller D, Koehler J, Birke K P. Low pressure glow-discharge methanation with an ancillary oxygen ion conductor. Journal of CO_2 Utilization, 2017, 19: 130–136
105. Aerts R, Somers W, Bogaerts A. Carbon dioxide splitting in a dielectric barrier discharge plasma: A combined experimental and computational study. ChemSusChem, 2015, 8(4): 702–716
106. Azzolina-Jury F, Thibault-Starzyk F. Mechanism of low pressure plasma-assisted CO_2 hydrogenation over Ni-USY by microsecond time-resolved FTIR spectroscopy. Topics in Catalysis, 2017, 60 (19): 1709–1721
107. Yan X L, Bao J H, Zhao B R, Yuan C, Hu T, Huang C F, Li Y N. CO dissociation on Ni/SiO_2: The formation of different carbon materials. Topics in Catalysis, 2017, 60(12-14): 890–897

108. Dai B, Gong W M, Zhang X L, Zhang L, He R. Studies on methanation of CO_2 under synergism plasma with catalyst. Chemical Journal of Chinese Universities, 2001, 22(5): 817–820 (in Chinese)

109. Jing L, Li Z H. Conversion of natural gas to C hydrocarbons via cold plasma technology. Journal of Energy Chemistry, 2010, 19(4): 375–379

110. Xu D J, Li Z H, Lv J, Wang B W, Xu G H. Methane conversion to C2 and higher hydrocarbons via dielectric-barrier discharge plasma at atmospheric pressure. Chemical Reaction Engineering & Technology, 2006, 22(4): 356–360

111. Lee D H, Song Y H, Kim K T, Lee J O. Comparative study of methane activation process by different plasma sources. Plasma Chemistry and Plasma Processing, 2013, 33(4): 647–661

112. Zhang X L, Di L B, Zhou Q. Methane conversion under cold plasma over Pd-containing ionic liquids immobilized on gamma-Al_2O_3. Journal of Energy Chemistry, 2013, 22(3): 446–450

113. Wilkes J S. A short history of ionic liquids-from molten salts to neoteric solvents. Green Chemistry, 2002, 4(2): 73–80

114. Nozaki T, Hattori A, Okazaki K. Partial oxidation of methane using a microscale non-equilibrium plasma reactor. Catalysis Today, 2004, 98(4): 607–616

115. Wang D W, Ma T C. Catalytic methane coupling of C2 hydrocarbons by glow discharge plasma. Nuclear Fusion and Plasma Physics, 2006, 4: 327–330 (in Chinese)

116. Goujard V, Tatibouët J M, Batiot-Dupeyrat C. Carbon dioxide reforming of methane using a dielectric barrier discharge reactor: Effect of helium dilution and kinetic model. Plasma Chemistry and Plasma Processing, 2011, 31(2): 315–325

117. Thanyachotpaiboon K, Chavadej S, Caldwell T A, Lobban L L, Mallinson R G. Conversion of methane to higher hydrocarbons in AC nonequilibrium plasmas. AIChE Journal. American Institute of Chemical Engineers, 1998, 44(10): 2252–2257

118. Zhang A J, Zhu A M, Guo J, Xu Y, Shi C. Conversion of greenhouse gases into syngas via combined effects of discharge activation and catalysis. Chemical Engineering Journal, 2010, 156 (3): 601–606

119. Jo S, Lee D H, Kang S, Song Y H. Methane activation using noble gases in a dielectric barrier discharge reactor. Physics of Plasmas, 2013, 20(8): 14–31

120. Jo S, Lee D H, Kim K T, Kang W S, Song Y H. Methane activation using Kr and Xe in a dielectric barrier discharge reactor. Physics of Plasmas, 2014, 21(10): 14–31

121. Sudnick J J, Corwin D L. VOC control techniques. Hazardous Waste & Hazardous Materials, 1994, 11(1): 129–143

122. Keller R A, Dyer J A. Abating halogenated VOCs. Chemical Engineering (Albany, N.Y.), 1998, 105(1): 100–105

123. Kim H H, Ogata A, Futamura S. Complete oxidation of volatile organic compounds (VOCs) using plasma-driven catalysis and oxygen plasma. International Journal of Plasma Environmental Science & Technology, 2007, 1: 46–51

124. Dyer J A, Mulholland K. Toxic air emissions. What is the full cost to your business? Chemical Engineering Environmental Engineering, 1994, 101 (S2): 4–8

125. Okubo M, Yamamoto T, Kuroki T, Fukumoto H. Electric air cleaner composed of nonthermal plasma reactor and electrostatic precipitator. IEEE Transactions on Industry Applications, 2001, 37 (5): 1505–1511

126. Chang C L, Lin T S. Decomposition of toluene and acetone in packed dielectric barrier discharge reactors. Plasma Chemistry and Plasma Processing, 2005, 25(3): 227–243

127. Ohshima T, Kondo T, Kitajima N, Sato M. Adsorption and plasma decomposition of gaseous acetaldehyde on fibrous activated carbon. IEEE Transactions on Industry Applications, 2010, 46 (1): 23–28

128. Vandenbroucke A, Mora M, Morent R, De Geyter N, Leys C. TCE abatement with a plasma-catalysis combined system using MnO_2 as catalyst. 21st International Symposium on Plasma Chemistry, 2013, 156: 94–100

129. Dinh M T N, Giraudon J M, Lamonier J F, Vandenbroucke A, De Geyter N, Leys C, Morent R. Plasma-catalysis of low TCE concentration in air using $LaMnO_{3+\delta}$ as catalyst. Applied Catalysis B: Environmental, 2014, 147(147): 904–911

130. Assadi A A, Bouzaza A, Vallet C, Wolbert D. Use of DBD plasma, photocatalysis, and combined DBD plasma/photocatalysis in a continuous annular reactor for isovaleraldehyde elimination-Synergetic effect and byproducts identification. Chemical Engineering Journal, 2014, 254(13): 124–132

131. Ogata A, Ito D, Mizuno K, Kushiyama S, Gal A, Yamamoto T. Effect of coexisting components on aromatic decomposition in a packed-bed plasma reactor. Applied Catalysis A, General, 2002, 236(1): 9–15

132. Yamamoto T, Mizuno K, Tamori I, Ogata A, Nifuku M, Michalska M, Prieto G. Catalysis-assisted plasma technology for carbon tetrachloride destruction. IEEE Transactions on Industry Applications, 1996, 32(1): 100–105

133. Ogata A, Yamanouchi K, Mizuno K, Kushiyama S, Yamamoto T. Oxidation of dilute benzene in an alumina hybrid plasma reactor at atmospheric pressure. Plasma Chemistry and Plasma Processing, 1999, 19(3): 383–394

134. Ogata A, Ito D, Mizuno K, Kushiyamaet S, Yamamoto T. Removal of dilute benzene using a zeolite-hybrid plasma reactor. IEEE Transactions on Industry Applications, 2001, 37(4): 959–964

135. Oh S M, Kim H H, Einaga H, Ogata A, Futamura S, Park D W. Zeolite-combined plasma reactor for decomposition of toluene. Thin Solid Films, 2006, 506-507: 418–422

136. Kuroki T, Hirai K, Matsuoka S, Kim J Y, Okubo M. Oxidation system of adsorbed VOCs on adsorbent using nonthermal plasma flow. IEEE Transactions on Industry Applications, 2011, 47(4): 1916–1921

137. Feng F D, Zheng Y Y, Shen X J, Zheng Q Z, Dai S L, Zhang X M, Huang Y F, Liu Z, Yan K P. Characteristics of back corona discharge in a honeycomb catalyst and its application for treatment of volatile organic compounds. Environmental Science & Technology, 2015, 49(11): 6831–6837

138. Sultana S, Vandenbroucke A M, Leys C, De Geyter N, Morent R. Abatement of VOCs with alternate adsorption and plasma-assisted regeneration: A review. Catalysts, 2015, 5(2): 718–746

139. Schiavon M, Torretta V, Casazza A, Ragazzi M. Non-thermal plasma as an innovative option for the abatement of volatile organic compounds: A review. Water, Air, and Soil Pollution, 2017, 228(10): 388

140. Vandenbroucke A M, Morent R, De Geyter N, Leys C. Non-thermal plasmas for non-catalytic and catalytic VOC abatement. Journal of Hazardous Materials, 2011, 195: 30–54
141. Feng X X, Liu H X, He C, Shen Z X, Wang T B. Synergistic effects and mechanism of a non-thermal plasma catalysis system in volatile organic compound removal: A review. Catalysis Science & Technology, 2018, 8(4): 936–954
142. Yang F, Li Y F, Liu T, Xu K, Zhang L Q, Xu C M, Gao J S. Plasma synthesis of Pd nanoparticles decorated-carbon nanotubes and its application in Suzuki reaction. Chemical Engineering Journal, 2013, 226: 52–58
143. Liang H F, Gandi A N, Anjum D H, Wang X B, Schwingenschlogl U, Alshareef H N. Plasma-assisted synthesis of NiCoP for efficient overall water splitting. Nano Letters, 2016, 16(12): 7718–7725
144. Wang S Y, Wang X Y, Wang L, Pu Q S, Du W B, Guo G S. Plasma-assisted alignment in the fabrication of microchannel-array-based in-tube solid-phase microextraction microchips packed with TiO_2 nanoparticles for phosphopeptide analysis. Analytica Chimica Acta, 2018, 1018: 70–77
145. Li S J, Li L L, Chen Z, Xue G P, Jiang L G, Zheng K, Chen J C, Li R, Yuan C, Huang M D. A novel purification procedure for recombinant human serum albumin expressed in *Pichia pastoris*. Protein Expression and Purification, 2018, 149: 37–42
146. Cong Z, Lee S. Study of mechanical behavior of BNNT-reinforced aluminum composites using molecular dynamics simulations. Composite Structures, 2018, 194: 80–86
147. Cogal S, Ela S E, Ali A K, Cogal G C, Micusik M, Omastova M, Oksuz A U. Polyfuran-based multi-walled carbon nanotubes and graphene nanocomposites as counter electrodes for dye-sensitized solar cells. Research on Chemical Intermediates, 2018, 44(5): 3325–3335
148. Qiu B, Yang C, Guo W H, Xu Y, Liang Z B, Ma D, Zou R Q. Highly dispersed Co-based Fischer-Tropsch synthesis catalysts from metal-organic frameworks. Journal of Materials Chemistry. A, Materials for Energy and Sustainability, 2017, 5(17): 8081–8086
149. Zhu L, Liu X Q, Jiang H L, Sun L B. Metal-organic frameworks for heterogeneous basic catalysis. Chemical Reviews, 2017, 117(12): 8129–8176
150. Jing P, Zhang S Y, Chen W J, Wang L, Shi W, Cheng P. A macroporous metal-organic framework with enhanced hydrophobicity for efficient oil adsorption. Chemistry-a European Journal, 2018, 24(15): 3754–3759
151. Carrasco J A, Romero J, Abellan G, Hernandez-Saz J, Molina S I, Marti-Gastaldo C, Coronado E. Small-pore driven high capacitance in a hierarchical carbon via carbonization of Ni-MOF-74 at low temperatures. Chemical Communications, 2016, 52(58): 9141–9144
152. Li Y Q, Gao Q, Zhang L J, Zhou Y S, Zhong Y X, Ying Y, Zhang M C, Huang C Q, Wang Y A. $H_5PV_2Mo_{10}O_{40}$ encapsulated in MIL-101(Cr): Facile synthesis and characterization of rationally designed composite materials for efficient decontamination of sulfur mustard. Dalton Transactions (Cambridge, England), 2018, 47(18): 6394–6403
153. Zhen W L, Li B, Lu G X, Ma J T. Enhancing catalytic activity and stability for CO_2 methanation on Ni@MOF-5 via control of active species dispersion. Chemical Communications, 2015, 51(9): 1728–1731
154. Li Y J, Miao J P, Sun X J, Xiao J, Li Y W, Wang H H, Xia Q B, Li Z. Mechanochemical synthesis of Cu-BTC@GO with enhanced water stability and toluene adsorption capacity. Chemical Engineering Journal, 2016, 298: 191–197
155. Zeng L, Xiao L, Long Y K, Shi X W. Trichloroacetic acid-modulated synthesis of polyoxometalate@UiO-66 for selective adsorption of cationic dyes. Journal of Colloid and Interface Science, 2018, 516: 274–283
156. Sadakiyo M, Yoshimaru S, Kasai H, Kato K, Takata M, Yamauchi M. A new approach for the facile preparation of metal-organic framework composites directly contacting with metal nanoparticles through arc plasma deposition. Chemical Communications, 2016, 52(54): 8385–8388
157. Park K S, Ni Z, Côté A P, Choi J Y, Huang R D, Uribe-Romo F J, Chae H K, O'Keeffe M, Yaghi O M. Exceptional chemical and thermal stability of zeolitic imidazolate frameworks. Proceedings of the National Academy of Sciences of the United States of America, 2006, 103(27): 10186–10191
158. Férey G, Mellot-Draznieks C, Serre C, Millange F, Dutour J, Surble S, Margiolaki I. A chromium terephthalate-based solid with unusually large pore volumes and surface area. Science, 2005, 309 (5743): 2040–2042
159. Kandiah M, Usseglio S, Svelle S, Olsbye U, Lillerud K P, Tilset M. Post-synthetic modification of the metal-organic framework compound UiO-66. Journal of Materials Chemistry, 2010, 20 (44): 9848–9851
160. Fujitani T, Nakamura I, Akita T, Okumura M, Haruta M. Hydrogen dissociation by gold clusters. Angewandte Chemie, 2009, 121(50): 9679–9682
161. Bahri M, Haghighat F, Rohani S, Kazemian H. Metal organic frameworks for gas-phase VOCs removal in a NTP-catalytic reactor. Chemical Engineering Journal, 2017, 320: 308–318
162. Li B H, Yu T H, Weng C Y, Yang C C, Lin C H, Lee S. Thermal and plasma synthesis of metal oxide nanoparticles from MOFs with SERS characterization. Vibrational Spectroscopy, 2016, 84: 146–152
163. Dou S, Dong C L, Hu Z, Huang Y C, Chen J L, Tao L, Yan D F, Chen D W, Shen C H, Chou S L, et al. Atomic-scale CoO_x species in metal-organic frameworks for oxygen evolution reaction. Advanced Functional Materials, 2017, 27(36): 1702546